PROTEINS: Structure, Function, and Genetics 17:337–346 (1993)

RESEARCH ARTICLES

Crystal Structure of *Escherichia coli* RNase HI in Complex With Mg^{2+} at 2.8 Å Resolution: Proof for a Single Mg^{2+}-Binding Site

Katsuo Katayanagi, Mika Okumura, and Kosuke Morikawa
Protein Engineering Research Institute, Osaka 565, Japan

ABSTRACT **To obtain more precise insight into the Mg^{2+}-binding site essential for RNase HI catalytic activity, we have determined the crystal structure of *E. coli* RNase HI in complex with Mg^{2+}. The analyzed cocrystal, which is not isomorphous with the Mg^{2+}-free crystal previously refined at 1.48 Å resolution, was grown at a high $MgSO_4$ concentration more than 100 mM so that even weakly bound Mg^{2+} sites could be identified. The structure was solved by the molecular replacement method, using the Mg^{2+}-free crystal structure as a search model, and was refined to give a final *R*-value of 0.190 for intensity data from 10 to 2.8 Å, using the XPLOR and PROLSQ programs. The backbone structures are in their entirety very similar to each other between the Mg^{2+}-bound and the metal-free crystals, except for minor regions in the enzyme interface with the DNA/RNA hybrid. The active center clearly revealed a single Mg^{2+} atom located at a position almost identical to that previously found by the soaking method. Although the two metal-ion mechanism had been suggested by another group (Yang, W., Hendrickson, W.A., Crouch, R.J., Satow, Y. Science 249:1398–1405, 1990) and partially supported by the crystallographic study of inactive HIV-1 RT RNase H fragment (Davies, J.F., II, Hostomska, Z., Hostomsky, Z., Jordan, S.R., Matthews, D. Science 252:88–95, 1991), the present result excludes the possibility that RNase HI requires two metal-binding sites for activity. In contrast to the features in the metal-free enzyme, the side chains of Asn-44 and Glu-48 are found to form coordinate bonds with Mg^{2+} in the metal-bound crystal.**

Key words: RNase H, Mg^{2+}-binding site, catalytic mechanism, molecular replacement

INTRODUCTION

Ribonuclease H (RNase H) specifically recognizes duplex DNA/RNA hybrids, and hydrolyzes only the RNA strand to produce 5′-phosphates.[1] *Escherichia coli* (*E. coli*) RNase H, which has been renamed RNase HI since the isolation of a second RNase H (RNase HII),[2] is the most precisely characterized enzyme in the RNase H family. This enzyme appears to participate in DNA replication in *E. coli*,[3–5] although its true physiological function still remains unclear. Retroviral replication requires RNase H activity,[6] and is carried by the RNase H component of the reverse transcriptase (RT).

Divalent metal ions are essential for RNase H activity. *E. coli* RNase HI requires Mg^{2+} for the activity, but in some cases, Mn^{2+} can be substituted.[7]

The crystal structure of *E. coli* RNase HI was determined by Katayanagi et al. at 1.8 Å resolution[8] and by Yang et al. at 2.0 Å resolution,[9] independently. The former group also identified the metal-binding site within the enzyme by soaking the crystals in Mg^{2+}, Ca^{2+}, and Ba^{2+} solutions constructing difference Fourier maps. A study of RNase H like sequences[10] revealed four invariant acidic residues that surround this single metal-binding site.[8] Combined with the results of site-directed mutagenesis experiments,[11] this feature of the metal-binding site suggested that at least some of these residues are directly involved in hydrolysis. Katayanagi et al. later reported the details of the structure–function relationships of the enzyme, which were based on the crystal structure refined at 1.48 Å resolution.[12]

Although the crystal structures of *E. coli* RNase

Abbreviations: RNase H, ribonuclease H; HIV, human immunodeficiency virus; RT, reverse transcriptase; NMR, nuclear magnetic resonance; rmsd, root mean square deviation; TAPS, *N*-tris (hydroxymethyl)methyl-3-aminopropanesulfonic acid; CHES, 2-(*N*-cyclohexylamino)-ethanesulfonic acid. Enzyme: ribonuclease H (EC 3.1.26.4).

Received April 19, 1993; revision accepted July 26, 1993.
Address reprint requests to Kosuke Morikawa, Protein Engineering Research Institute, 6-2-3 Furuedai, Suita, Osaka 565, Japan.

HI reported by the two groups were essentially identical, the interpretations of the catalytic mechanism were somewhat different. For instance, Yang et al. raised the possibility that the nucleolytic activity of *E. coli* RNase HI requires two divalent metal ions and four carboxylates,[9] like the 3'-5'-exonuclease activity of DNA polymerase I,[13,14] although definite experimental proof could not be provided. Later, Davies et al. reported the crystal structure of the human immunodeficiency virus-1 (HIV-1) RT RNase H domain determined at 2.4 Å resolution.[15] On the basis of the difference Fourier map calculated from the derivative crystal, prepared by soaking in a Mn^{2+} solution, they also reported that the HIV-1 RNase H domain contains the two Mn^{2+} sites located near the position corresponding to the Mg^{2+} site in *E. coli* RNase HI. However, the soaking method is sometimes unreliable for making a definite conclusion about ligand-binding, because the difference Fourier maps are prone to produce uninterpretable densities arising from local conformational changes. Furthermore, an NMR study[16] was carried out to evaluate the alkaline earth metal-binding site and the binding constants of *E. coli* RNase HI with the metals in solution. In agreement with the crystallographic results,[8,12,17] the Hill plot analyses of the NMR signals revealed that all the alkaline earth metals, such as Mg^{2+}, Ca^{2+}, and Ba^{2+}, bind to one single site in the enzyme.

In order to provide a more definite conclusion, we have produced an Mg^{2+}–*E. coli* RNase HI cocrystal at a high concentration of Mg^{2+} and have determined its crystal structure at 2.8 Å resolution. The refined structure provides evidence that *E. coli* RNase HI binds only one single Mg^{2+} cation at a position identical to that previously identified by soaking. It also reveals that the side chains of some residues around the active site alter their conformations to form coordinate bonds with the metal.

MATERIALS AND METHODS

Crystallization

The cocrystallization of *E. coli* RNase HI with Mg^{2+} was carried out under high Mg^{2+} concentrations to allow identification of metals even weakly bound to the enzyme. The crystals were grown in drops initially containing 3.6 mg/ml protein, 90–100 mM $MgSO_4$, 50 mM TAPS + CHES (pH 8.2–8.9), and 25% saturated $(NH_4)_2SO_4$, using the hanging drop mode of the vapor diffusion technique. These drops were initially equilibrated with a 45% saturated $(NH_4)_2SO_4$ solution, and later its reservoir concentration was gradually increased to about 65% saturation over a few weeks time. It should be noted that the Mg^{2+} concentration exceeded 100 mM when crystals appeared in the crystallization drops. The typical crystal has a thin tetragonal cylinder-like shape with dimensions of 60 × 60 × 450 μm.

TABLE I. Conditions of the Data Collection

Crystal size (μm)	60 × 60 × 450
Rotation axis	c*
Beam current (mA)	285–280
Wave length (Å)	1.00
Camera radius (mm)	286.5
Colimator (mm)	0.1
Oscilation angle (°)	7.98
Omega overlap (deg)	0.48
Camera movement (mm)	2.28
Coupling constant (°/mm)	3.5
Rotation speed (°/sec)	2.0
Number of oscillations	12
Exposure time (sec/film)	47.88
Number of films	11
No. of reflections	
Observed	15,785
Unique	3,953
R_{merge}	0.095
Resolution (Å)	2.8
Completeness (%)	90.1

Data Collection

Preliminary crystal data were determined using a precession camera (Enraf-Nonius) installed on a RU300 rotating anode generator (Rigaku Ltd). Afterward, synchrotron radiation was used to confirm that the crystals belonged to the space group $P4_122$ or $P4_322$ with unit cell parameters $a = b = 63.2$ Å and $c = 80.6$ Å. The unit cell contains one 17,559 Da protein molecule per asymmetric unit. The V_m values of the crystal and the water content were calculated to be 2.29 and 0.463, respectively.

The crystal size was not large enough to collect intensity data using conventional laboratory-level X-ray facilities, and hence the intensity data were collected using a Weissenberg camera for macromolecules,[18] which is installed at the beamline 6A2 in Photon Factory (Tsukuba, Japan). The camera radius was set at 286.5 mm. Diffraction patterns, recorded on an imaging plate (Fuji Film), were digitalized using the reading system BA100 (Fuji Film). The beam current varied from 285 to 280 mA, and the wavelength was fixed at 1.00 Å. All data collections were carried out at 15°C. To avoid the scattering of the diffracted beam by air, the helium gas was constantly flowing into a sealed area comprising the collimator, the crystal, and the detector. The conditions for data collection are summarized in Table I.

The intensity data were processed using the program system WEIS.[19] The Lorentz polarization factor correction, scaling, and merging between each film were carried out using this program. The reflections with $F > 1\sigma(F)$ were used for structural determinations, and the R_{merge} based on the intensity was 9.5%. The resolution for refinement was determined from a Wilson plot to be 2.8 Å. In total, 15,785 observed reflections were merged to 3,953

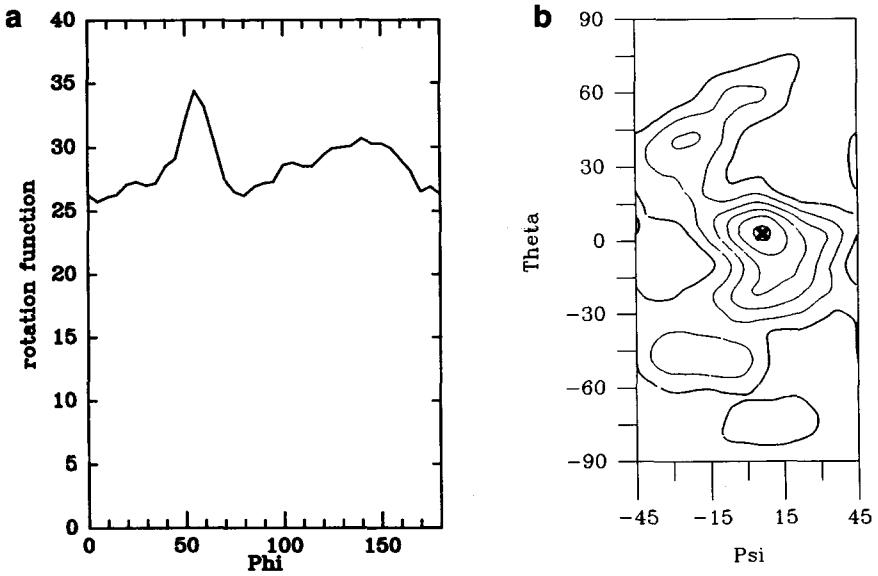

Fig. 1. Rotation function of the Mg^{2+}-RNase HI cocrystal. (**a**) The maximal values in each ϕ-layer. (**b**) The (ψ, θ) distribution at the maximal ϕ-layer, ϕ = 56.0°. The map is contoured in arbitrary steps. The significant primary solution (marked by cross) is shown.

unique reflections with a degree of completeness of 90.1%.

Structure Determination

Initial phases for the structure factors were obtained using the molecular replacement method. The metal-free structure of *E. coli* RNase HI refined at 1.48 Å resolution,[12] which was deposited at the Brookhaven Protein Data Bank[20] as 2RN2, was used as a starting model for the molecular search. This model was placed into a hypothetical triclinic cell with lattice parameters $a = b = c = 80$ Å and $\alpha = \beta = \gamma = 90°$. The rotational patterson search was performed using the program PROTEIN.[21] First, with the origin fixed at the center of gravity in the triclinic lattice, the Patterson functions were calculated from both the observed and the calculated structure factors from 10 to 3 Å resolution. The rotation search was initially carried out with an angle increment of 5° in a region of ($0°<\psi<90°$, $0°<\theta<180°$, $0°<\phi<180°$), with angles defined by R. Huber. The overall B value was assumed as 15.0 Å^2. After a possible peak for the solution was found, a finer increment of 1.0° or 0.2° was applied to determine more accurate rotation angles. A vector search, based on the calculated 1,946 Patterson peaks, was carried out. The limits for the Patterson search were set to 8–15 Å to exclude cross-vectors. A significant peak was observed at (ψ, θ, ϕ) = (6.0°, 4.0°, 56.0°). Figure 1 shows the distribution of the maximum rotation functions within each ϕ-layer and the distribution in the (ψ, θ) plane at the highest ϕ-layer.

Using the determined orientation matrix, the translation function formulated by Crowther and Blow[22] was calculated, using the program originally written by E.E. Lattman and later modified by J. Deisenhofer and R. Huber. Among all the translation vectors, only one significant peak was found which was derived from the $P4_322$ symmetry operation. However, a consistent peak of translation vectors could not be found from the $P4_122$ operation. Thus, the enantiomorph was determined to be $P4_322$ rather than $P4_122$. The correct translation value determined is (X, Y, Z) = (−19.85 Å, 3.46 Å, 0.00 Å). The observed peaks corresponding to the respective translation vectors are summarized in Table II. In the model deduced from the rotation and translation search results, the molecular packing within the crystal lattice is reasonable, and yields no collision between the neighboring molecules, except for the loop region around His-124. At this stage, the structure factors were calculated with an R-factor of 39.2% for reflections from 10.0 to 3.0 Å resolution. The $(2|F_o|-|F_c|)$ difference Fourier map showed continuous electron densities, and the boundary between the protein and the solvent regions was clear.

Crystallographic Refinement

To adjust the molecular orientation and position more accurately, a rigid body refinement was applied using the program TRAREF.[23] After 7 cycles, the rotation and translation values of this model were slightly shifted. After the movement, the corrected values for rotation and translation were (ψ, θ, ϕ) = (−0.28°, −0.62°, 1.05°) and (X, Y, Z) = (0.16 Å, 0.0 Å, −0.08 Å), respectively. The R-factor for the

TABLE II. Solution of the Translation Function

Translation vector	Harker section	Peak height	Peak position		
			u	v	w
$(2x,2y,1/2)$	$w=1/2$	7.1σ	0.3694	0.1067	0.5001
$(x+y,y-x,1/4)$	$w=1/4$	9.7σ	0.7423	0.3703	0.2489
$(x-y,x+y,3/4)$	$w=3/4$	9.6σ	0.6295	0.7425	0.7511
$(2x,0,2z)$	$v=0$	10.9σ	0.3720	0.0000	0.0000
$(0,2y,2z-1/2)$	$u=0$	10.0σ	0.0000	0.1092	0.4993
$(x-y,y-x,2z+3/4)$		8.7σ	0.6325	0.3675	0.7478
$(x+y,x+y,2z+1/4)$		5.4σ	0.7377	0.7379	0.2500

data from 10 to 3.0 Å resolution also decreased to 38.1%.

The initial model was then improved to fit a $(2|F_o|-|F_c|)$ difference Fourier map, using the interactive graphics program FRODO[24] on a PS300 (Evans & Sutherland) display system. A restrained least-square refinement was subsequently carried out using the program PROLSQ.[25] Upon convergence, the R-factor was decreased to 24.4% for intensity data from 10 to 3.0 Å resolution. However, the quality of the electron density map at this stage was not satisfactory. Therefore, a further refinement, using the molecular dynamics refinement program XPLOR,[26] was carried out for intensity data to 2.8 Å resolution, while omitting the Mg^{2+} coordinates. After this refinement which was calculated according to the protocol of "heatstage" at 3,000 K and "slow cooling" from 4,000 K to 300 K, the R-factor was converged to 22.5%. Next, the PROLSQ program was reapplied for some cycles of refinement again. Thus, the quality of the electron density map was obviously improved. At this stage, the Mg^{2+} position was clearly identified in both Mg^{2+} deleted difference Fourier maps with the respective coefficients of $(2|F_o|-|F_c|)$ and $(|F_o|-|F_c|)$ (omit map). After the R-factor reached 21.5%, 35 water molecules were identified in the map. The refinement was continued to include the coordinates of these water molecules and the Mg^{2+} cation. At this stage, the R-factor was 20.4% for the 3,834 reflections between 10 and 2.8 Å resolution. Individual temperature factors of protein atoms were finally refined with tight restraints. The R-factor was thus converged to 19.0%. The final refinement statistics are summarized in Table III.

RESULTS AND DISCUSSION

Overall Structure

As shown in Figure 2 (a) and (b), the overall backbone structures are almost the same between the Mg^{2+}-free and Mg^{2+}-bound *E. coli* RNase HI, whereas the molecular arrangements in the two crystal forms are different. The rmsd value calculated from the Cα coordinates was 0.92 Å between the two structures. Compared with the metal-free enzyme, only three loops, Arg-27–Lys-33, Thr-92–Lys-96, and Gly-123–Pro-128, in the Mg^{2+}-bound enzyme exhibit slight but significant conformational differences. The glycine rich region[12] ranging from Gly-11 to Gly-23 also shows a smaller conformational change than these three loops. All of these differences can be reasonably explained by the crystal packing effects. Yang et al.[9] reported that a sulfate ion is bound with full occupancy at a position near the NH_2-termini of helices I and IV which is 13.7 Å away from the center of the carboxyl triad formed by Asp-10, Glu-48, and Asp-70. It is likely that this same sulfate ion is observed in the structure of the Mg^{2+}-bound enzyme, since its cocrystal was grown at a high concentration of sulfate ion. However, we could not find an electron density corresponding to the sulfate ion in the map. This discrepancy is presumably due to a local structural difference around its binding site which is associated with slightly different molecular arrangements between the two crystals. In this Mg^{2+}-RNase HI cocrystal, the two side chains of Asn-45, which belong to two neighboring molecules, make a polar interaction through two water molecules. Presumably, this intermolecular interaction blocks the sulfate ion binding.

Mg^{2+}-Coordination

In the previous reports[8,12] we described the single Mg^{2+} position which was found from the difference Fourier map with the coefficient $(|F(Mg^{2+}\text{-bound})|-|F(Mg^{2+}\text{-free})|)\exp(i\varphi_{MIR})$ by using the soaking method. In order to make the metal position more convincing, two other heavier alkaline earth metals, Ca^{2+} and Ba^{2+}, were also introduced by soaking in the metal-free crystal to produce the difference Fourier map. Both metals, which significantly facilitate the enzymic activity of RNase HI (S. Iwai et al., in preparation), were located at a position identical to that of Mg^{2+}.

The present X-ray structural analysis of the Mg^{2+}-RNase HI cocrystal provides a definite experimental proof for the existence of only one metal-binding site, because a cocrystal grown in an equilibrium state can avoid producing artifact of electron densities which sometimes lead to misinterpretations in the use of the soaking method.

TABLE III. Final Refinement Statistics

Restraints	rmsd	(σ)
Distance		
Bond length (Å)	0.017	(0.020)
Angle related (Å)	0.044	(0.030)
Planar (Å)	0.056	(0.050)
Planar groups (Å^2)	0.013	(0.020)
Chiral volumes (Å^3)	0.199	(0.150)
Nonbonded contacts		
Single torsion (Å)	0.222	(0.300)
Multiple torsion (Å)	0.263	(0.300)
Possible H-bond (Å)	0.260	(0.300)
Torsion angles		
Peptide plane (ω)	2.4	(3.0)
Staggerd (± 60 or 180°)	25.2	(15.0)
Orthonormal (± 90°)	31.8	(20.0)
Isotropic thermal factors		
Main-chain bond (Å^2)	0.765	(1.500)
Main-chain angle (Å^2)	1.281	(2.000)
Side-chain bond (Å^2)	1.061	(2.000)
Side-chain angle (Å^2)	1.593	(2.500)

As shown in Figure 3, the Mg^{2+}-deleted difference Fourier map clearly reveals a single Mg^{2+} atom bound at almost the same position as previously identified by soaking in the metal-free enzyme.[8,12] The peak height of the electron density indicates approximately full occupancy of the Mg^{2+} cation. This single metal-binding site in RNase HI is consistent with the results from a solution NMR metal-binding study.[16] Furthermore, NMR (Y. Oda, personal communication) and crystallographic studies (M. Ishikawa et al., in preparation) revealed that the addition of mononucleotides or a few trinucleotide pairs with complementary sequences cannot facilitate metal-binding. This result suggests that the enzyme binds the metal cations at this single site, regardless of the presence or the absence of nucleic acids. Therefore, we conclude that a single divalent metal is essential for the catalytic activity of RNase HI.

In contrast to this finding of the single metal-binding site, Davies et al.[15] reported, on the basis of soaking experiments, that the HIV-1 RT RNase H domain binds two Mn^{2+} cations, although this isolated domain shows no RNase H activity in vitro. Their soaking experiments used a much higher concentration (45 mM) of the Mn^{2+} transition metal cation than the maximum 10 mM of alkaline earth metal used for *E. coli* RNase HI. We suggest the possibility that this high concentration of Mn^{2+} may result in the insignificant secondary Mn^{2+} site, since Mn^{2+} has a much stronger tendency of forming coordinate bonds than any other alkaline earth metals. Furthermore, site-directed mutagenesis experiments[11] have shown that Asp-134 in RNase HI is not essential for the activity. This finding is inconsistent with the hypothesis that RNase HI and the HIV-1 RT RNase H domain require a second metal-binding site for activity,[9] because the corresponding Asp participates in the second Mn^{2+}-binding within the HIV-1 RT RNase H domain.[15]

Schematic representations of the Mg^{2+}-free and Mg^{2+}-bound crystal structures are shown in Figure 4. The torsion angles of the residues involved in Mg^{2+}-binding are summarized in Table IV.

In the Mg^{2+}-free enzyme, the two carboxyl groups of Asp-10 and Glu-48 are 5.2 Å away from each other, because of electrostatic repulsion. The carboxyl group of Glu-48 is fixed by forming hydrogen bonds with two neighboring residues, Asn-44 and Ser-71.[12] Furthermore, one water molecule (W250) is located at the empty metal position, instead of Mg^{2+}, and presumably it cancels the repulsion in the empty Mg^{2+}-binding site.

The refined structure of RNase HI complexed with Mg^{2+} revealed that the side chains of Glu-48 and Asn-44 move by 1.48 and 1.87 Å as compared to those in the metal-free crystal, respectively, and form coordinate bonds with the metal cation, while the conformations of Asp-10 and Gly-11, which also coordinate with Mg^{2+}, remain the same as those found in the metal-free enzyme.[12]

We have collected the diffraction data at 2.0 Å resolution from crystals soaked in a 10 mM $MgCl_2$ solution (data not shown). Using the coordinates of the Mg^{2+}-free crystal refined by Katayanagi et al.,[12] we have calculated the $(2|F_o|-|F_c|)$ and $(|F_o|-|F_c|)$ difference Fourier maps (omit maps) which were phased excluding the coordinates of Asp-10, Gly-11, Asn-44, Glu-48, Asp-70, and Asp-134. The omit maps show obvious movements of these side chains. These side chain movements are very similar to those found in the Mg^{2+}-RNase HI cocrystal, although the magnitudes of the movements are smaller in the soaked crystal than in the cocrystal, because of a lower occupancy of Mg^{2+} in the soaked crystal. This result also supports that the Mg^{2+} cation and the surrounding protein atoms were correctly identified in the cocrystal. Furthermore, we have examined the positions of the two Mn^{2+} cations found in the HIV-1 RT RNase H fragment crystal,[15] but no significant electron density was found around the corresponding sites in the Mg^{2+}-RNase HI cocrystal.

The distances from Mg^{2+} to Asp-70–Oδ1, Asp-70–Oδ2, and Asp-134–Oδ1 are 4.44, 4.89, and 5.36 Å, respectively. These values are almost the same as those in the Mg^{2+}-free crystal. Due to the 2.8 Å resolution of the structural analysis, we could identify smaller numbers of water molecules in the Mg^{2+}-bound crystal than in the Mg^{2+}-free crystal. However, we presume that many water molecules would be located near the Mg^{2+}-binding site. In any case, it appears that there is enough empty space around the Mg^{2+} to accommodate phosphate groups during hydrolysis. It is thus likely that the bound

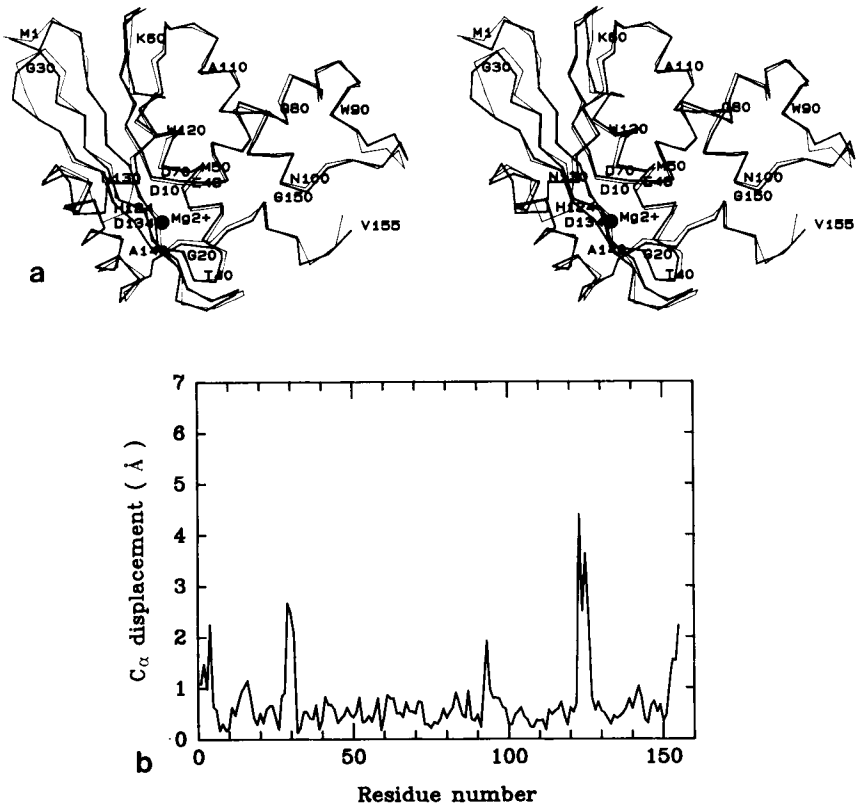

Fig. 2. Comparison of the overall structures. (**a**) Stereo pair of the Cα backbone superimposed between Mg^{2+}-free (thin) and Mg^{2+}-bound (thick) RNase HI. (**b**) Cα-coordinate shifts of the Mg^{2+}-bound enzyme, as compared to the Mg^{2+}-free enzyme. The secondary structures are defined as follows[12]: αI (43–58), αII (71–79), αIII (81–89), αIV (100–112) αV (127–141), βA (5–14), βB (19–28), βC (31–39), βD (63–69), and βE (115–121).

TABLE IV. Comparison of Torsion Angles Between the Mg^{2+}-Free (Upper) and the Mg^{2+}-Bound Enzymes (Lower)

Mg^{2+}	Asp-10	Gly-11	Asn-44	Glu-48	Asp-70	Asp-134
Free						
ψ	−154	−139	−57	−69	−101	−58
ϕ	154	151	−41	−33	5	−50
χ1	−156		−150	173	69	−174
χ2	−7		97	173	−8	22
χ3				5		
Bound						
ψ	−170	−179	−67	−78	−89	−59
ϕ	178	132	−45	−41	−52	−58
χ1	−149		−161	−151	78	−170
χ2	−26		26	−145	−71	60
χ3				−89		

Mg^{2+} is sandwiched between the enzyme and the nucleic acid.

An Mg^{2+} cation is usually coordinated to six ligands with an octahedral symmetry. Four residues, Asp-10, Gly-11, Gly-48, and Asn-44, are directly coordinated with Mg^{2+}, while Asp-70 and Asp-134 seem to make electrostatic interactions with the metal cation. These six residues are oriented in appropriate directions for octahedral coordination. However, some phosphates of the DNA/RNA hybrid could also occupy positions for coordination. A structural determination of the enzyme in complex with a DNA/RNA hybrid will provide more detailed insight into the coordination.

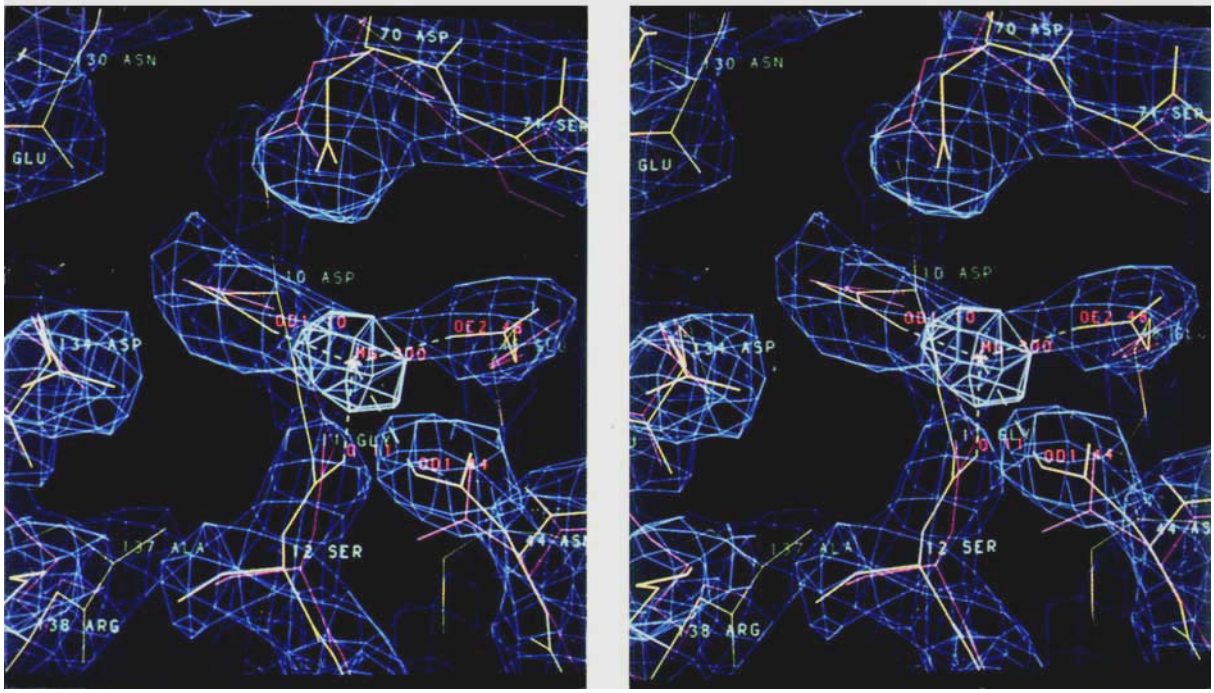

Fig. 3. ($2|F_o| - |F_c|$) difference Fourier map (blue) of Mg^{2+}-bound RNase HI which is contoured at 1.0 σ level. The yellow and pink backbones indicate the Mg^{2+}-bound and the Mg^{2+}-free enzyme, respectively. The Mg^{2+}-deleted ($|F_o| - |F_c|$) difference Fourier map (omit map) in light blue indicates a single Mg^{2+} cation. For this phase calculation, only the Mg^{2+} coordinates were eliminated. The peak height of the Mg^{2+} cation is 4.5 σ.

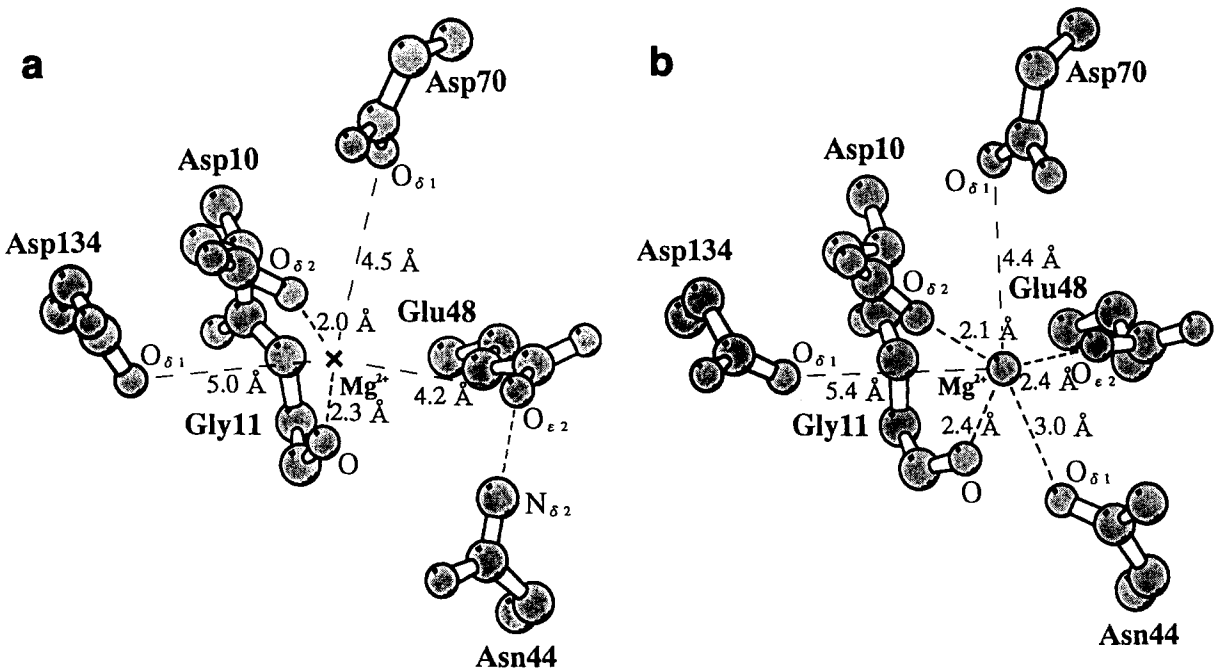

Fig. 4. Three dimensional structure of the active center. (**a**) Active site of the metal-free enzyme and the Mg^{2+} position introduced into the crystal by the soaking method. (**b**) Active site of the Mg^{2+}-bound enzyme.

Catalytic Mechanism

A hydrolytic mechanism for *E. coli* RNase HI, which is different from the two divalent metal ion mechanism,[9,13,14] has been proposed, on the basis of the crystal structure and an NMR analysis.[27] This hydrolysis scheme is similar to that for DNase

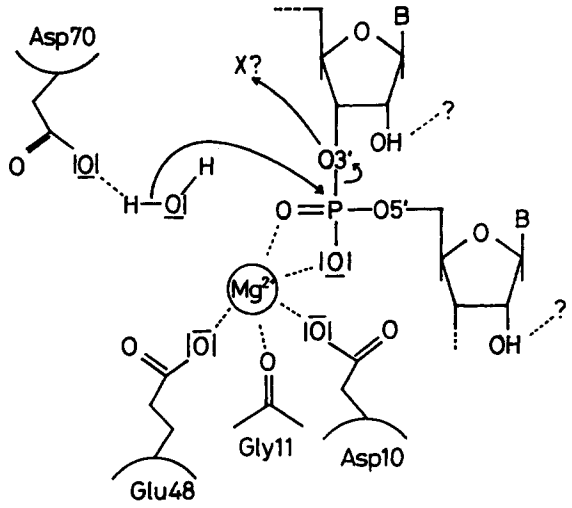

Fig. 5. Revised scheme of the catalytic reaction of the *E. coli* RNase HI. The X? mark indicates an unknown proton-donating residue. The ? marks indicate putative residues interacting with RNA.

I,[28–30] which also contains a single metal cation binding site essential for the activity.

The conformational changes of the active site residues as described in the previous section, and, in particular, the side chain movement of Glu-48 upon Mg^{2+} coordination, are generally consistent with the structural features of the three active site mutants, D10N (replacing Asp-10 by Asn), E48Q and D70N.[31] Analyses of these mutant structures suggest that the three carboxyl groups, Asp-10, Glu-48, and Asp-70, are electrostatically repulsive in the absence of Mg^{2+}, and hence that Mg^{2+}-binding to the enzyme induces a conformational change in the active site by cancelling the negative charges of the carboxyl groups. This also implies that the major role of Mg^{2+}-binding may be to shift the catalytic groups from unfavorable to favorable positions for hydrolysis.

Which hydrolytic scheme can be proposed from the present data? We assume that a single Mg^{2+} cation, coordinated by the side chains of Asp-10 and Glu-48 as well as the main chain carbonyl group of Gly-11, correctly positions the scissile phosphate backbone for hydrolysis (Fig. 5), that is, a role similar to that proposed for Ca^{2+} in DNase I.[28–30] It is most likely that the carboxyl group of Asp-70 activates a water molecule which attacks the phosphorous atom in a nucleophilic manner. These interpretations are consistent with the results from site-directed mutagenesis.[11] It is more difficult to assign a functional group which donates a proton at the end of the catalytic reaction. It seems to us that the side chain of His-124 is a reasonable candidate, although its replacement by alanine did not completely abolish the activity.[11] Recently, on the basis of results by NMR and site-directed mutagenesis, another role of His-124 has been proposed.[32] It is also a possible catalytic mechanism in which, as suggested for the restriction enzymes, *Eco*RI and *Eco*RV,[33] the 3′-phosphate group of the DNA/RNA hybrid activates the attacking water, instead of an amino acid of the enzyme. The carboxyl group of Asp-70 may then play a role as a proton donor.

Crystal Packing

As reported previously,[8] the RNase HI molecule has a remarkably biased charge distribution. Therefore, when crystals are grown in the absence of divalent metal cations, protein molecules are arranged within the crystal lattice to cancel their biased charges. In fact, in the metal-free crystal, the acidic Mg^{2+}-binding cavity is buried by the basic protrusion. In more detail, the Lys87-Nζ of the neighboring molecule approaches Asp-10–Oδ1 (2.81 Å) and Asp-70–Oδ2 (2.57 Å).[12] These intermolecular electrostatic interactions prevent the introduction of mononucleotides or oligonucleotides into the crystals by soaking. The crystal of RNase H from *Thermus thermophilus* HB8[34] also has a packing scheme similar to that of *E. coli* RNase HI, although the *T. thermophilus* RNase H crystal belongs to the $P6_522$ space group which is different from the $P2_12_12_1$ space group of the *E. coli* RNase HI crystal.

The molecular arrangement in the Mg^{2+}-bound RNase HI crystal is represented in Figure 6. In contrast to the packing in the metal-free crystal, the Mg^{2+}-binding cavity of the enzyme faces the long solvent region extending along four fold screw axis (z-axis). Because of the resolution limit (2.8 Å) of the present structural analysis, only 35 water molecules could be identified in the Mg^{2+}-bound crystal. However, the results of Mg^{2+}-free crystal at 1.48 Å resolution[12] suggest that many water molecules are assumed to lie in this region and cancel the biased charge distribution.

CONCLUSIONS

The present X-ray crystallographic analysis of Mg^{2+}-bound RNase HI reveals that *E. coli* RNase HI contains a single Mg^{2+}-binding site essential for the activity. This finding consequently excludes the possibility that the hydrolysis by RNase HI and RT RNase H domains proceeds through the two divalent metal ion mechanism, such as that proposed for the 3′-5′-exonuclease activity of DNA polymerase I.[13,14] On the basis of the new coordination scheme between the Mg^{2+} and the surrounding functional groups, we have proposed a hydrolytic reaction scheme that has slightly revised the previously reported pathways.[27] Furthermore, it should be noted that the Mg^{2+}-bound crystal is suitable for investigating the interactions of the enzyme with nucleic acids, because the Mg^{2+}-binding site faces the large solvent region and is accessible to various oligonucleotides introduced into the crystal.

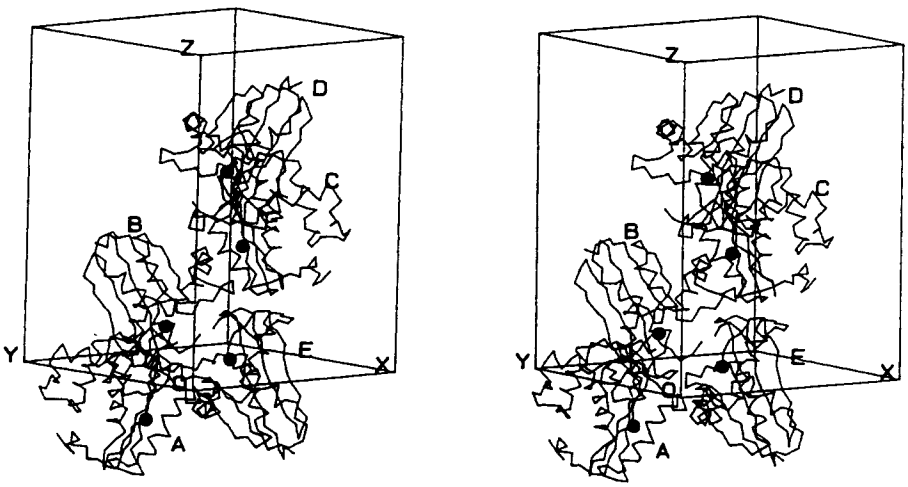

Fig. 6. Crystal packing of the Mg^{2+}-bound *E. coli* RNase HI. The bound Mg^{2+} cations are indicated by filled circles. Molecules A, B, C, and D are arranged along the 4-fold screw axis which coincides with the *z*-axis. Molecule E is related with C by 2-fold axis perpendicular to the *z*-axis. The distance of the two Mg^{2+} cations, which belong to B and E, respectively, is 17.4 Å.

ACKNOWLEDGMENTS

We are grateful to Drs. S. Kanaya, H. Nakamura, and Y. Oda for their helpful discussions and comments, and to Professor N. Sakabe, Dr. A. Nakagawa, Mr. T. Shimizu, Ms. M. Ariyoshi, and Mr. K. Ishikawa for their assistance in data collection at the Photon Factory (Tsukuba). Ms. T. Hashimoto is acknowledged for the purification of *E. coli* RNase HI. We also appreciate Dr. A. Pähler for his critical reading of the manuscript. M.O. was financially supported by a grant for international collaboration groups from the Human Frontier Science Program.

REFERENCES

1. Linn, S. M., Roberts, R. J. (eds.). Ribonuclease H. In: "Nuclease." Cold Spring Harbor, NY: Cold Spring Harbor Laboratory, 1982:211–241.
2. Itaya, M. Isolation and characterization of a second RNase H (RNase HII) of *Escherichia coli* K-12 encoded by the *rnhB* gene. Proc. Natl. Acad. Sci. U.S.A. 87:8587–8591, 1990.
3. Itoh, T., Tomizawa, J.-I. Formation of an RNA primer for initiation of replication of ColE1 DNA by ribonuclease H. Proc. Nat. Acad. Sci. U.S.A. 77:2450–2454, 1980.
4. Horiuchi, T., Maki, H., Sekiguchi, M. RNase-H-defective mutants of *Escherichia coli:* A possible discriminatory role of RNase H in initiation of DNA replication. Mol. Gen. Genet. 195:17–22, 1985.
5. Dasgupta, S., Masukata, H., Tomizawa, J.-I. Multiple mechanisms for initiation of ColE1 DNA replication: DNA synthesis in the presence and absence of ribonuclease H. Cell 51:1113–1122, 1987.
6. Varmus, H. Retroviruses. Science 240:1427–1435, 1988.
7. Berkower, I., Leis, J., Hurwitz, J. Isolation and characterization of an endonuclease from *Escherichia coli* specific for ribonucleic acid in ribonucleic acid-deoxyribonucleic acid hybrid structures. J. Biol. Chem. 248:5914–5921, 1973.
8. Katayanagi, K., Miyagawa, M., Ishikawa, M., Matsushima, M., Kanaya, S., Ikehara, M., Matsuzaki, T., Morikawa, K. Three-dimensional structure of ribonuclease H from *E. coli*. Nature (London) 347:306–309, 1990.
9. Yang, W., Hendrickson, W. A., Crouch, R. J., Satow, Y. Structure of ribonuclease H phased at 2 Å resolution by MAD analysis of the selenomethionyl protein. Science 249: 1398–1405, 1990.
10. Doolittle, R. F., Feng, D.-F., Johnson, M. S., McClure, M. A. Origins and evolutionary relationships of retroviruses. Quart. Rev. Biol. 64:1–30, 1989.
11. Kanaya, S., Kohara, A., Miura, Y., Sekiguchi, A., Iwai, S., Inoue, H., Ohtsuka, E., Ikehara, M. Identification of the amino acid residues involved in an active site of *Escherichia coli* ribonuclease H by site-directed mutagenesis. J. Biol. Chem. 265:4615–4621, 1990.
12. Katayanagi, K., Miyagawa, M., Matsushima, M., Ishikawa, M., Kanaya, S., Nakamura, H., Ikehara, M., Matsuzaki, T., Morikawa, K. Structural details of ribonuclease H from *Escherichia coli* as refined to an atomic resolution. J. Mol. Biol. 223:1029–1052, 1992.
13. Freemont, P. S., Friedman, J. M., Beese, L. S., Sanderson, M. R., Steitz, T. A. Cocrystal structure of an editing complex of Klenow fragment with DNA. Proc. Natl. Acad. Sci. U.S.A. 85:8924–8928, 1988.
14. Beese L. S., Steitz, T. A. Structural basis for the 3′–5′ exonuclease activity of *Escherichia coli* DNA polymerase I: a two metal ion mechanism. EMBO. J. 10:25–33, 1991.
15. Davies, J. F., II, Hostomska, Z., Hostomsky, Z., Jordan, S.R., Matthews, D. Crystal structure of the ribonuclease H domain of HIV-I reverse transcriptase. Science 252:88–95, 1991.
16. Oda, Y., Nakamura, H., Kanaya, S., Ikehara, M. Binding of metal ions to *E. coli* RNase HI observed by ^{1}H-^{15}N heteronuclear 2D NMR. J. Biomolec. NMR 1:247–255, 1991.
17. Morikawa, K., Katayanagi, K. RNase H: Three-dimensional structure and function. Bull. Inst. Pasteur 90:71–82, 1992.
18. Sakabe, N. X-ray diffraction data collection system for modern protein crystallography with a Weissenberg camera and an imaging plate using syncrotron radiation. Nucl. Instrum. Methods Phys. Res. Sect. A 303:448–463, 1991.
19. Higashi, T. The processing of diffraction data taken on a screenless Weissenberg camera for macromolecular crystallography. J. Appl. Crystallogr. 22:9–18, 1989.
20. Bernstein, F. C., Koetzle, T. F., Williams, G. J., Meyer, E. E. J., Brice, M. D., Rodgers, J. R., Kennard, O., Shimanouchi, T., Tsumi, M. The protein data bank: A computer-based archival file for macromolecular structures. J. Mol. Biol. 112:535–542, 1977.
21. Steigemann, W. Die Entwicklung und Anwendung von Rechenverfahren und Rechenprogrammen zur Strukturanalyse von Proteinen am Beispiel des Trypsin-Trypsininhibitor Komplexes, des freien Inhibitors und der L-Aspa-

raginase. Ph. D. thesis, Technical University of Munich, Germany, 1974.
22. Crowther, R. A., Blow, D. M. A method of positioning a known molecule in an unknown crystal structure. Acta Crystallogr. 23:544–548, 1967.
23. Huber, R., Schneider, M. A group refinement procedure in protein crystallography using Fourier transforms. J. Appl. Crystallogr. 18:165–169, 1985.
24. Jones, T. A. A graphics model building and refinement system for macromolecules. J. Appl. Crystallogr. 11:268–272, 1978.
25. Hendrickson, W. A. Stereochemically restrained refinement of macromolecular structures. Methods Enzymol. 115:252–270, 1985.
26. Brünger, A. T., Kurian, J., Karplus, M. Crystallographic R factor refinement by molecular dynamics. Science 235: 458–460, 1987.
27. Nakamura, H., Oda, Y., Iwai, S., Inoue, H., Ohtsuka, E., Kanaya, S., Kimura, S., Katsuda, C., Katayanagi, K., Morikawa, K., Miyashiro, H., Ikehara, M. How does RNase H recognize a DNA/RNA hybrid? Proc. Natl. Acad. Sci. U.S.A. 88:11535–11539, 1991.
28. Suck, D., Oefner, C., Kabsch, W. Three-dimensional structure of bovine pancreatic DNase I at 2.5 Å resolution. EMBO J. 3:2423–2430, 1984.
29. Suck, D., Oefner, C. Structure of DNase I at 2.0A resolution suggests a mechanism for binding to and cutting DNA. Nature (London) 321:620–625, 1986.
30. Weston, S. A., Lahm, A., Suck, D. X-ray structure of the DNase I-d(GGTATACC)$_2$ complex at 2.3 Å resolution. J. Mol. Biol. 26:1237–1256, 1992.
31. Katayanagi, K., Ishikawa, M., Okumura, M., Ariyoshi, M., Kanaya, S., Kawano, Y., Suzuki, M., Tanaka, I., Morikawa, K. Crystal structures of ribonuclease HI active site mutants from *Escherichia coli*. J. Biol. Chem., 268:22092–22099, 1993.
32. Oda, Y., Yoshida, M., Kanaya, S. Role of histidine 124 in the catalytic function of ribonuclease HI from *Escherichia coli*. J. Biol. Chem. 268:88–92, 1993.
33. Jeltsch, A., Alves, J., Maass, G., Pingoud, A. On the catalytic mechanism of *Eco*RI and *Eco*RV: A detailed proposal based on biochemical results, structural data and molecular modelling. FEBS Lett. 304:4–8, 1992.
34. Ishikawa, K., Okumura, M., Katayanagi, K., Kimura, S., Kanaya, S., Nakamura, H., Morikawa, K. Crystal structure of ribonuclease H from *Thermus thermophilus* HB8 refined at 2.8 Å resolution. J. Mol. Biol. 230:529–542, 1993.